In Situ Monitoring of the Reaction-Induced Self-Assembly of Phenolic Resin Templated by Diblock Copolymers

Jheng-Guang Li, Wei-Cheng Chu, U.-Ser Jeng, Shiao-Wei Kuo*

In this study, in situ small-angle X-ray scattering (SAXS), in situ Fourier transform infrared (FTIR) spectroscopy, and transmission electron microscopy (TEM) are used to monitor the formation of ordered mesophases in cured mixtures of phenolic resin and the diblock copolymer poly(ethylene oxide-*block*-ε-caprolactone) (PEO-*b*-PCL). SAXS and TEM analyses reveal that the mesophase of the phenolic/PEO-*b*-PCL mixture transforms sequentially from disordered to short-range-ordered to hexagonal-cylindrical to gyroidal during the curing process when using hexamethylenetetramine (HMTA) as a cross-linking agent, indicating that a mechanism involving reaction-induced microphase separation controls the self-assembly of the phenolic resin. In situ SAXS is also used to observe the fabrication of mesoporous phenolic resins during subsequent calcination processes.

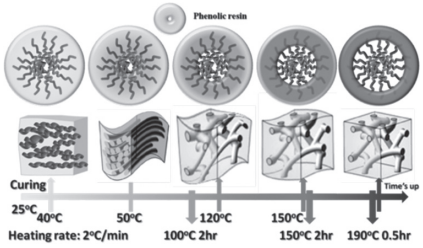

1. Introduction

The preparation of mesoporous phenolic resins and carbons through organic–organic self-assembly has received much attention because these materials have a wide range of potential applications.[1–21] Phenolic resins can be divided into two classes: resol- and novolac-based materials.[22–24] Resol-type nanostructures can form phenolic thermosets in the absence of any additives during the curing process. Accordingly, using a resol as a carbon precursor for the one-step synthesis of mesoporous carbons through thermal treatment under a N_2 atmosphere can be an efficiency strategy; nevertheless, mesoporous resol-based materials typically lack thermal stability because of their lower degrees of cross-linking. Notably, however, Ikkala and co-workers[7] and Ruokolainen and co-workers[8] prepared mesoporous phenolic resins templated by poly(isoprene-*block*-2-vinylpyridine)[25] and poly(styrene-*block*-4-vinylpyridine) diblock copolymers with hexamethylenetetramine (HMTA) as the curing agent to fabricate thermally stable mesoporous phenolic resins.

In previous studies, we used evaporation-induced self-assembly (EISA), with double-crystalline poly(ethylene oxide-*block*-ε-caprolactone) (PEO-*b*-PCL) diblock copolymers as templates and HMTA as the crosslinking agent, to prepare a series of mesoporous phenolic resins.[3–5] In these phenolic resin/PEO-*b*-PCL systems, we observed, using small-angle X-ray scattering (SAXS), transmission electron microscopy (TEM), differential scanning calorimetry (DSC), and Fourier transform infrared (FTIR) spectroscopy, an interesting relationship between the transformation of the mesophase and the degree of competitive hydrogen bonding. Furthermore, blending of PEO–POSS [Star poly(ethylene oxide)–functionalized silsesquioxane] during the preparation process could result in so-called disorder–order and order–order transitions by enhancing the long-range ordering and the mesophase transformation, respectively.[3] Although several other key factors are known to affect the mesophase formation during the EISA process, including the interaction of the interface and the rate of solvent evaporation,[26–28] the subsequent

Dr. J.-G. Li, W.-C. Chu, Prof. S.-W. Kuo
Department of Materials and Optoelectronic Science,
Center for Nanoscience and Nanotechnology,
National Sun Yat-Sen University, Kaohsiung 804, Taiwan
E-mail: kuosw@faculty.nsysu.edu.tw
Dr. U.-S. Jeng
National Synchrotron Radiation Research Center, Hsin-Chu Science Park, Taiwan.

DOI: 10.1002/macp.201300332

crosslinking (or curing) steps of these complicated mixtures have rarely been investigated, especially through in situ observation of the curing process.

In this study, we used in situ FTIR spectroscopy, in situ SAXS, and TEM measurements to determine that thermal treatment is the most important factor affecting the mesophase of phenolic/PEO-*b*-PCL mixtures. In a typical procedure, we used in situ SAXS and FTIR spectroscopy to monitor the curing of a mixed thin film of PEO-*b*-PCL diblock copolymer ($EO_{114}CL_{84}$; $\overline{M}_n$ = 14 580 g mol^{-1}), novolac-phenolic resin, and HMTA obtained after EISA processing. The in situ SAXS data revealed a surprising phenomenon: the mesostructure of the mixture transformed sequentially from a disordered structure to a short-range ordered structure to a hexagonal cylindrical structure and finally to a bicontinuous phase (gyroid) structure upon thermal curing; this behavior was consistent with the corresponding TEM observations. In addition, in situ FTIR spectroscopy revealed that the degree of hydrogen bonding of the phenolic/PCL pair gradually decreased upon extending the curing process (or increasing the temperature), indicating that the cross-linked phenolic resin gradually distributed to the outer regions of the structure as its molecular weight increased during the curing procedure (Scheme 1).

2. Experimental Section

2.1. Materials

The double-crystalline block copolymer PEO-PCL ($EO_{114}CL_{84}$) was synthesized through ring-opening polymerization, with a molecular weight of 14 580 g mol^{-1} (determined using ^{1}H NMR spectroscopy) and 22 000 g mol^{-1} and a polydispersity index (PDI) of 1.31 [determined using gel permeation spectroscopy (GPC) with DMF as the eluent (0.6 mL min^{-1}) and calibration with polystyrene (PS) standards]. Star PEO–POSS was purchased from Hybrid Plastics (USA) with a molecular weight of 5576 g mol^{-1}. The phenolic was synthesized through a condensation reaction with H_2SO_4, producing an average molecular weight ($\overline{M}_n$ = 500 g mol^{-1}) similar to those described in previous studies.[3–5]

2.2. Preparation of Uncured Thin Films and Mesoporous Phenolic Thin Films

Phenolic resin, HMTA, and PEO-*b*-PCL (for the preparation of phenolic resin/PEO-*b*-PCL/HMTA thin films at a weight ratio of 50:50:5 or phenolic resin/PEO-*b*-PCL/PEO-POSS/HMTA thin films at a weight ratio of 50:50:22:5) were dissolved in THF until the solution became homogeneous. The THF was evaporated slowly at room temperature and then the sample was vacuum-dried at 30 °C for 1 d to obtain the uncured thin film. Curing of the samples was performed under the following temperature profile: 100 °C for 2 h, then 150 °C for 2 h, and then 190 °C for 0.5 h. The cross-linked samples were pyrolyzed through slow heating of the samples from room temperature to 330 °C at a rate of 1 °C min^{-1} in the absence of a protective gas.[4]

2.3. Characterization

Thermal analysis was performed using a TA Instruments Q-20 differential scanning calorimeter operated at a heating rate of 20 °C min^{-1} and a cooling rate of 5 °C min^{-1} over a specific temperature range under N_2. In situ FTIR spectra of the samples were recorded using the uncured thin film and a Bruker Tensor 27 FTIR spectrophotometer. IR spectra recorded at elevated temperatures by

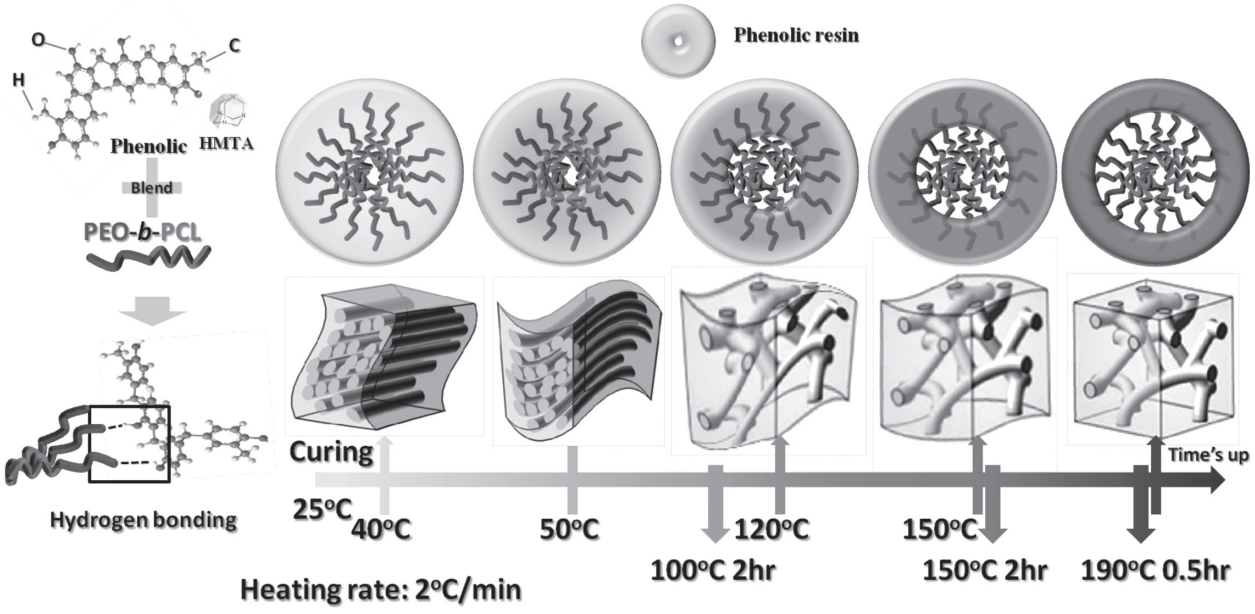

Scheme 1. Preparation and mesophase transformations of a phenolic resin/PEO-*b*-PCL mixture during the curing process.

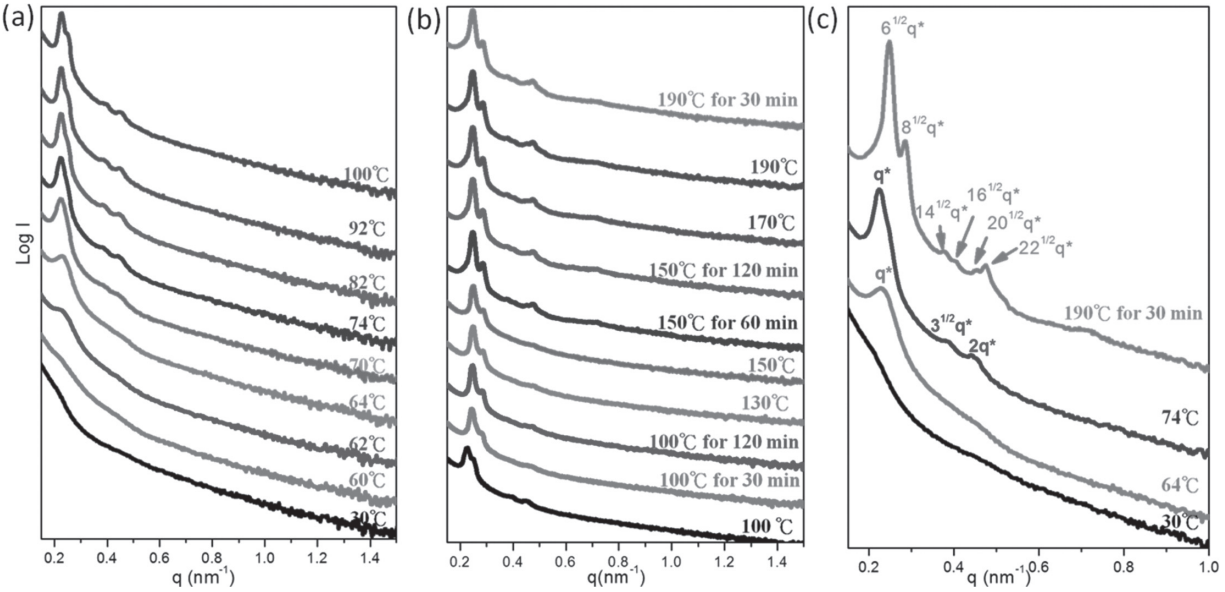

Figure 1. a,b) In situ SAXS patterns of the phenolic resin/PEO-*b*-PCL mixture during the curing reaction; c)Selected SAXS patterns of the specific phenolic resin/PEO-*b*-PCL mixture.

similar curing stages of phenolic resins were obtained by using a cell mounted inside the temperature-controlled compartment of the spectrometer. In situ SAXS experiments were performed using the SWAXS instrument at the BL17B3 beamline of the NSRRC, Taiwan; the X-ray beam had a diameter of 0.5 mm and a wavelength (λ) of 1.24 Å; *d*-spacings were calculated using the formula, $d = 2\pi/q$, where q is the scattering vector. All temperature-resolved SAXS measurements were carried out at several temperatures by similar curing stages of phenolic resins on a hot-stage under a dry nitrogen atmosphere. TEM images were recorded using a JEOL 3010 microscope (Japan) operated at 200 kV; samples were prepared through solution-casting without thermal annealing.

3. Results and Discussion

Figure 1 displays in situ SAXS experimental data recorded during various curing periods to obtain kinetic SAXS data (that is, treating the sample at 100 °C for 2 h, at 150 °C for 2 h, and at 190 °C for 30 min with a temperature increasing rate of 2 °C min^{-1}). These kinetic SAXS measurements reveal extremely different patterns that can be distinguished into roughly three periods: a first period from 30 to 70 °C (Figure 1a) in which the SAXS patterns reveal a transformation from disorder to short-range order (single peak); a second period between 70 and 100 °C (Figure 1a) in which an interesting feature could be observed: the single scattering peak tended toward a set of specific peaks in a ratio (1:√3:√4) that indicated the development of representative hexagonal cylindrical packing; and a final key period from 100 °C to the end of the cross-linking reaction (Figure 1b) in which the set of SAXS peaks changed from a ratio of 1:√3:√4 to √6:√8:√14:√16:√20, illustrating that the mesophase of the phenolic resin/PEO-*b*-PCL mixture gradually transformed from hexagonal cylindrical packing to a bicontinuous packing (gyroid) structure, a so-called order–order transition. The brief summary in Figure 1c reveals that the blend mixture featured a disordered arrangement at the onset of curing (30 °C). When the curing temperature reached over 60 °C, the single-scattering peak suddenly appeared, revealing that the crystalline properties of the PEO and PCL segments are both close to 60 °C greatly affected the mesophase of the mixture; we attribute this phenomenon to two effects: a rapid increase in electron density contrast and a sudden increase in the mixture's mobility, leading to microphase separation–induced self-assembly behavior when the curing temperature was above the melting point of double-crystalline PEO-*b*-PCL. Continuing the curing process up to a temperature of 74 °C, the SAXS pattern revealed clear hexagonal cylindrical packing, resulting in the SAXS profile exhibiting organized peaks at a peak ratio of 1:√3:√4. However, the broad main peak of SAXS data shows it contain a side peak at 74 °C, therefore, we believe it should be the mixed structure of hexagonal packing and gyroid, or the transition structure with two kinds of structure characters. When we completed the curing reaction at 190 °C for 30 min, we obtained a final phenolic resin/PEO-*b*-PCL product exhibiting typical gyroid character (Scheme 1). The order–order phase transformation occurs during the curing process. As the system evolved from hexagonal cylinder to gyroid with higher surface areas, we suggest one mechanism: the interfaces become gradually softened due to the diminishing hydrogen bonding at

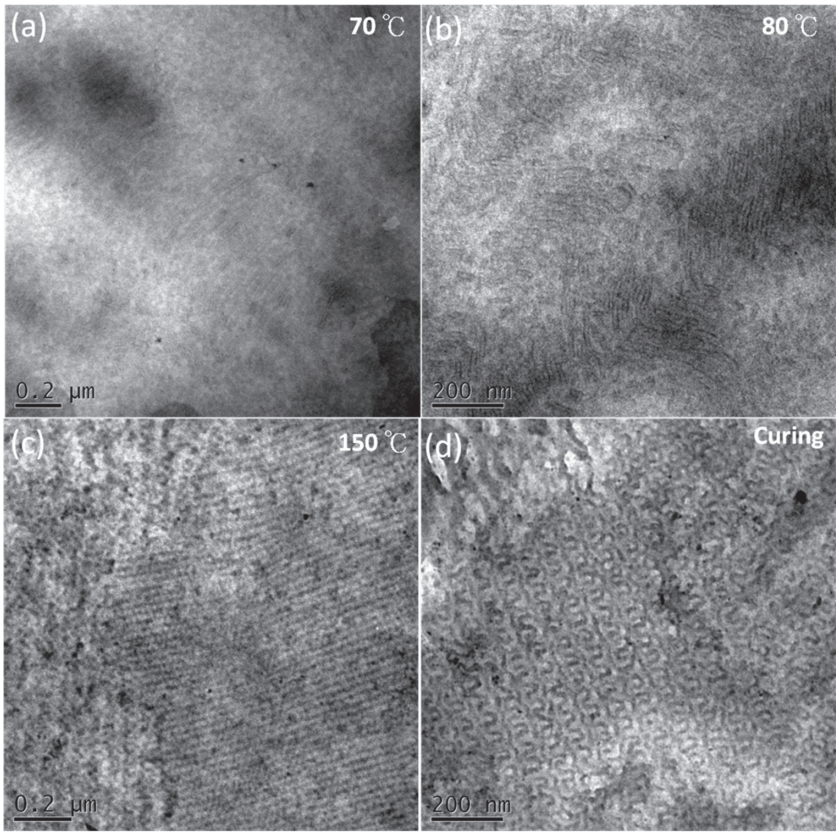

Figure 2. Selected microtomed TEM images of the specific phenolic resin/PEO-*b*-PCL mixture during the curing reaction.

elevated temperatures (lower surface energy owing to the lost of hydrogen bonding). Which may trigger the transformation for gyroid; before the phenolic cross-linked (high surface energy again). We assume the system may need to anneal at 100–120 °C for formation of gyroid, and cure (or cross-linked) the structure at a higher temperature, such as 150 °C. Therefore, the structure is locked due to extremely high rigid surfaces (or rod shells).

To confirm these SAXS results, we used TEM to characterize the cured phenolic resin/PEO-*b*-PCL mixture. Figure 2 displays TEM images of selected cured thermosets at 70, 80, and 150 °C and the final product. The side view images in Figure 2a,b reveal that hexagonal cylindrical packing was maintained until the curing temperature reached above 70 °C. Our SAXS characterization revealed that the mesophase of the phenolic resin/PEO-*b*-PCL mixture gradually transformed from a cylindrical to gyroidal structure when the curing temperature reached above 100 °C; the TEM image in Figure 2c reveals a clear cubic character, providing further evidence for the mesophase indeed changing to a gyroid type at 150 °C. The final product of curing reaction also exhibited a gyroid structure, as evidenced in Figure 2d, although the TEM images of the above-mentioned four cured samples displayed poor contrast, due to the low difference in electron density between the phenolic resins and our PEO-*b*-PCL template. The combination of SAXS and TEM characterization confirmed that an apparent mesophase transformation—from disordered to short-range ordered to cylindrical and finally to gyroidal—occurred during the curing process. Thus, this event is not only the first direct observation of a mesophase transition but also provides powerful evidence for thermal treatment (cross-linking reactions) indeed being a key factor in the reaction-induced self-assembly of the final mesophase of the phenolic resin/PEO-*b*-PCL (matrix/template) mixture.[29]

To determine the variations in hydrogen bonding and the distribution of phenolic resin during the curing process, we recorded in situ FTIR spectra of the C=O stretching region (from 1770 to 1670 cm^{-1}) of the phenolic resin/PEO-*b*-PCL/HMTA mixture (Figure 3), knowing that both the ether groups of the PEO blocks and the C=O groups of the PCL blocks are capable of interacting with the OH groups of the phenolic resin through intermolecular hydrogen bonding. The signal for the C=O stretching of the phenolic/PEO-*b*-PCL/HMTA system was split into two bands—for the free and hydrogen-bonded C=O groups, respectively—that fitted well to the Gaussian function. In Figures 3a,b, we observe two separate C=O stretching bands from the curing range from 30 to 100 °C for 120 min, corresponding to the hydrogen-bonded (1708 cm^{-1}) and free (1734 cm^{-1}) C=O groups, respectively, of the PCL segments in the PEO-*b*-PCL block copolymers. The fraction of hydrogen-bonded C=O groups decreased upon increasing the curing temperature, suggesting that the cured phenolic resin tended to distribute at the outer regions of the film upon increasing the progress of the cross-linking reaction (i.e., increasing the molecular weight of the cured phenolic resins), due to lower solubility and the weaker interactions between the C=O groups of the PCL segments and the OH groups of the phenolic resin (Scheme 1); accordingly, the inter-association equilibrium constant for the OH/ether oxygen atom interaction (K_A = 264) was greater than that for the OH/O=C interaction (K_A = 116) at room temperature.[30,31] Figure 3c further reveals that when the curing temperature was maintained beyond 100 °C, the curing-phenolic resin had left the PCL domain entirely, because only the signal for free C=O appeared in the FTIR spectra. The

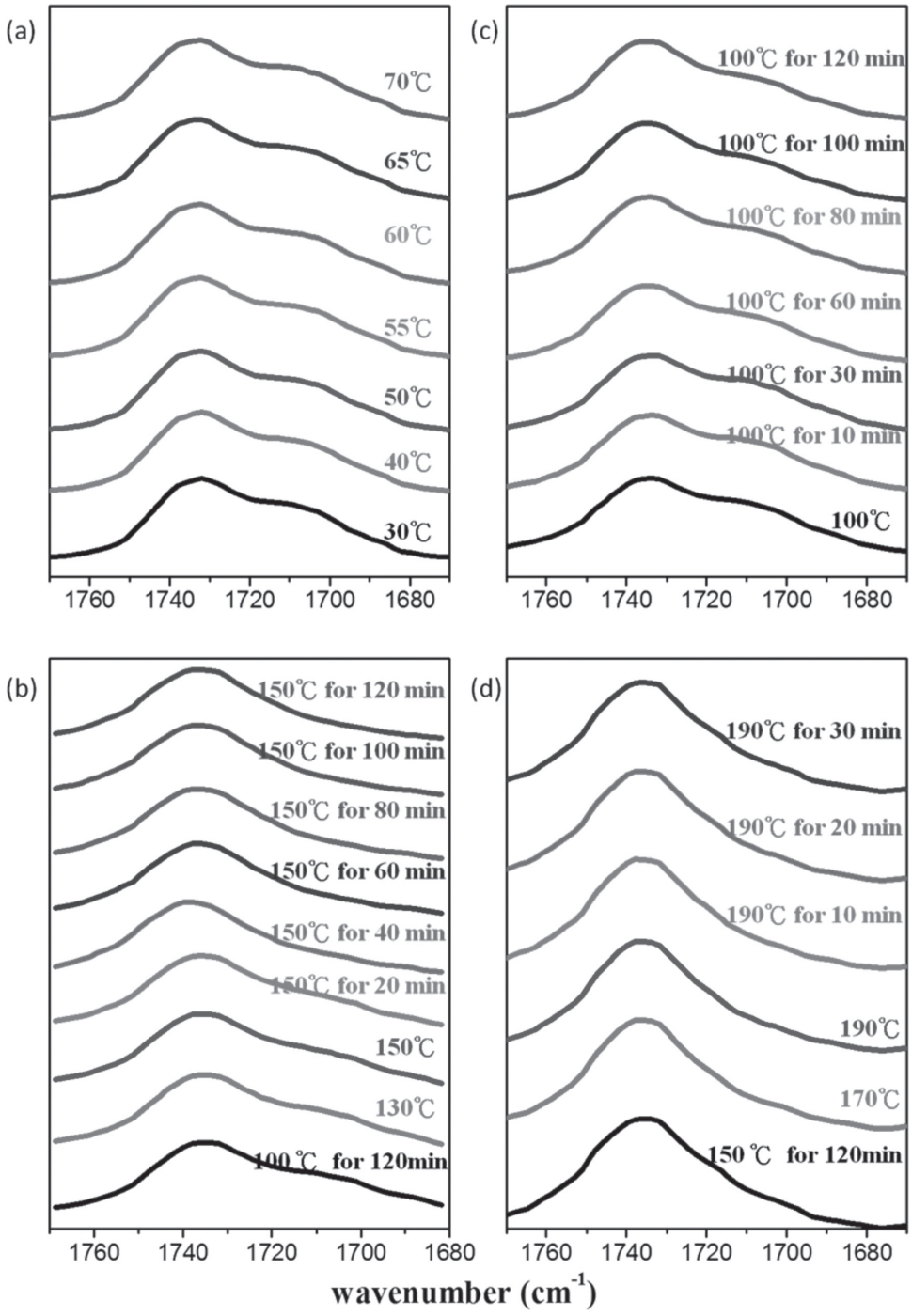

Figure 3. In situ FTIR spectra of the phenolic resin/PEO-*b*-PCL mixture during the curing reaction.

fraction of hydrogen-bonded C=O groups can be calculated using an appropriate absorptivity ratio ($\alpha_R = \alpha_{HB}/\alpha_F$ = 1.5), as we have discussed extensively in a previous study.[30] The curve fitting data revealed that the ratio of hydrogen-bonded C=O groups decreased between the beginning and the end of the curing process (32.8% initially, close to 0% ultimately). Our experimental FTIR spectra suggest that the fraction of hydrogen-bonded C=O groups of the PCL block decreased upon increasing the temperature, consistent with the SAXS patterns and TEM images; thus, the blend material underwent a transformation to a complete gyroid structure while the phenolic resins units were expunged from the PCL domains. Figure 3d displays FTIR spectra recorded after the curing step, revealing that the final gyroid structure had been fabricated completely to become the stable mesophase,

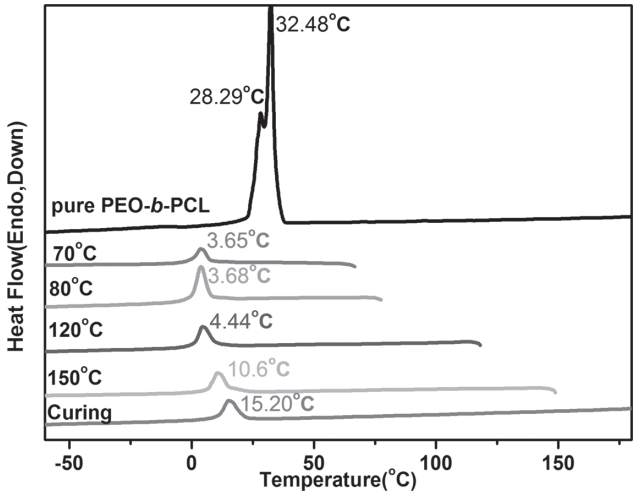

Figure 4. DSC cooling curves of the phenolic/PEO-*b*-PCL mixture after specific curing periods.

consistent with the SAXS data. On the basis of previous experiments, we propose that the phenolic resins gradually migrated to the outer domains of the self-assembled structure, forming an increasingly denser phase, during the disordered-to-cylindrical and cylindrical-to-gyroidal transition processes (Scheme 1).

Figure 4 presents DSC traces of the cured phenolic resin/PEO–PCL mixture recorded during the cooling scan under specific conditions. The peak temperature of the crystallization exotherm is defined as the freezing temperature (T_f); a higher value of T_f corresponds to a faster rate of crystallization. Previous studies have found that the value of T_f is associated with nonisothermal crystallization under a fixed cooling rate and that it displays a distinct correlation with the microdomain structure.[32,33] The DSC cooling curve of the pure PEO-*b*-PCL block copolymer exhibited two separate and low values of T_f, due to the restricted movement of the two blocks of the copolymer, relative to those of the pure homopolymers PEO and PCL; the higher value of T_f represents the crystallization of PEO and the other, lower value to the contribution of crystalline PCL.[5] As is evident in Figure 4, the value of T_f shifted unexpectedly to higher temperature when the curing temperature was greater than 120 °C, indicating the effect of confinement of the copolymer suddenly decreased when the mesophase transformed from cylindrical to gyroidal, based on the lower degree of restriction of the bicontinuous structure, consistent with the SAXS and TEM data. Finally, after performing the whole curing process, we used calcination to remove the PEO-*b*-PCL template and construct mesoporous phenolic resins. The in situ SAXS experiment revealed during the calcination process (Figure 5a) that the higher-ordering reflection peak become sharper as a result of the removal of PEO-*b*-PCL, leading to pore formation and greater contrast in electron density. Figure 5b displays the SAXS pattern of the final pyrolyzed product; its characteristic √6:√8:√14:√16:√20:√22 reflection ratio confirms that a clear gyroidal structure remained after calcinations. The primary SAXS scattering located in 0.25 nm^{-1}, which √6q^* indicated the reflection viewed from [211], the *d*-spacing could be calculated to 25 nm, and the cell parameter "*a*" could be calculated to 61 nm by the equation $a = 6^{1/2}d_{211}$. In addition, we used TEM analysis to confirm the structural ordering and bicontinuous symmetry of this material (Figure 5c–e). The TEM images of the gyroid-type mesoporous phenolic resin with different orientations ([111], [110], and [311] planes, respectively) were consistent with a bicontinuous-gyroid structure having $Ia\bar{3}d$ symmetry. Besides, we could directly measure the parameter "*a*" (approximately 59 nm) from the TEM image of [111] direction in Figure 5c, this result also nearly agreed with the cell parameter obtained from the SAXS primary reflection (d_{211} = 25 nm and *a* = 61 nm).

We observed a similar phenomenon in another blending system—phenolic resin/PEO-*b*-PCL/PEO-POSS/HMTA—in a previous report, where the final calcined product exhibited hexagonal cylindrical packing.[3] Hence, we applied in situ SAXS characterization also to that system to observe its timely mesophase transformation (Figures 6 and 7). Figure 6 displays the SAXS patterns recorded during the curing process; similar to the phenolic resin/PEO-*b*-PCL system, the mesophase transformed from disordered to short-range ordered beyond the melting point (ca. 60 °C, Figure 6a), progressed to a hexagonal cylindrical structure (ca. 100 °C, Figure 6a), and eventually formed a stable hexagonal cylindrical structure providing the definitive 1:√3:2 ratio of its scattering peaks (>150 °C, Figure 6b). Figure 7a presents the SAXS patterns (Figure 7a) of this phenolic resin mixture at the onset of the calcination process; it exhibits three apparent reflections with a 1:√3:2 reflection ratio, corresponding to a hexagonal cylindrical structure. TEM images (Figure 7b,c) of the calcined product viewed from the [001] (top view of cylinder, Figure 7b) and [10] (side view of cylinder, Figure 7c) directions, respectively, were consistent with a hexagonal cylindrical structure (2D).

4. Conclusion

To observe the range of mesophase transformations occurring during curing and calcination processes, we used SAXS, FTIR, TEM, and DSC to perform a series of in situ characterizations of phenolic/PEO-*b*-PCL and phenolic/PEO-*b*-PCL/PEO-POSS mixtures. SAXS and TEM analyses revealed that the mesophase of the phenolic/PEO-*b*-PCL mixture transformed from disordered to short-range ordered to hexagonal cylindrical and, finally, to gyroidal structures

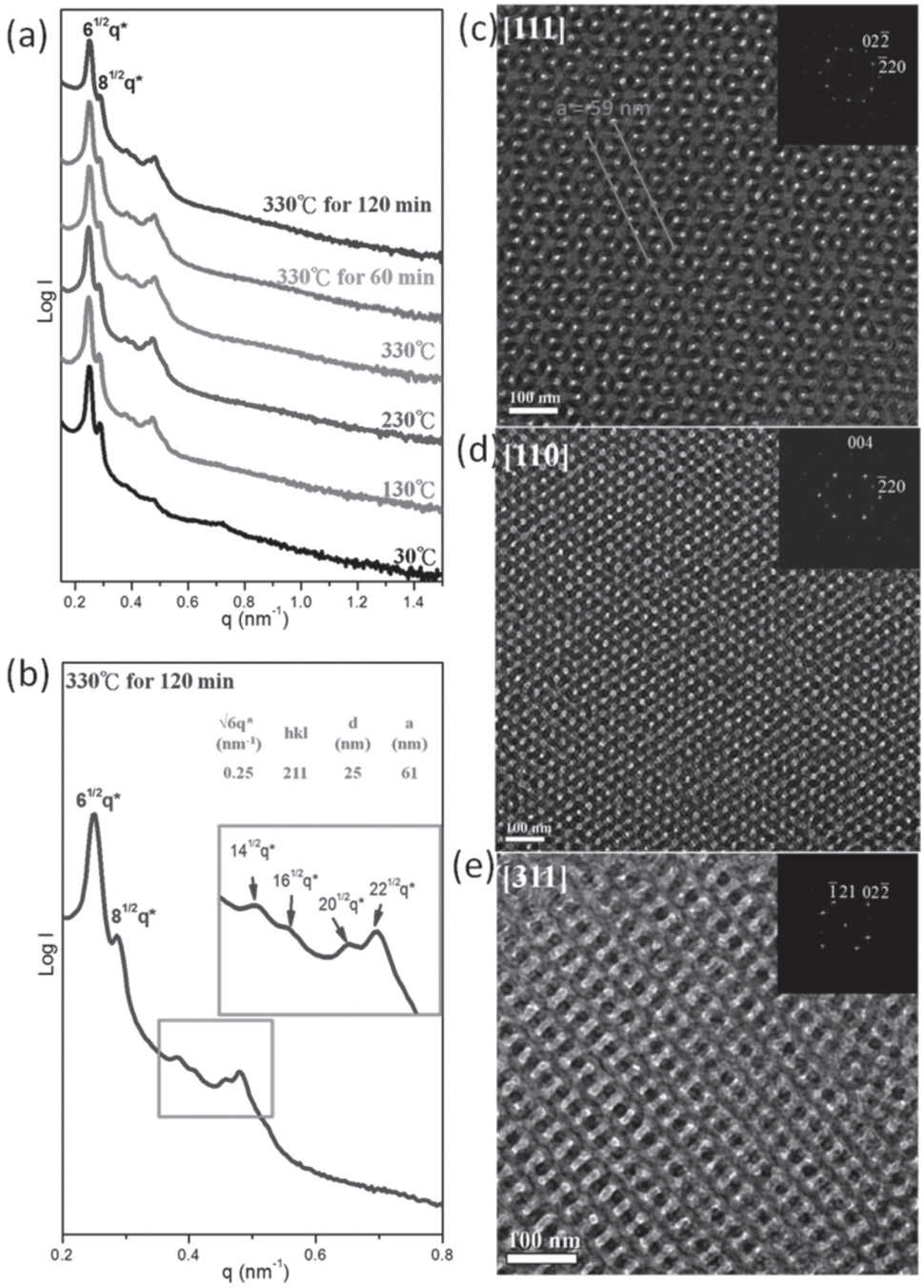

Figure 5. a) In situ SAXS patterns of the cured phenolic resin/PEO-*b*-PCL mixture during the calcination process. b) SAXS pattern of the mesoporous phenolic resin obtained after calcination. c–e) TEM images of the gyroidal mesoporous phenolic resin viewed along the [111], [110], and [311] planes, respectively.

during the curing procedure; similar phenomena occurred in the phenolic/PEO-*b*-PCL/PEO-POSS mixture, with the mesostructure of the mixture changing from disordered to short-range ordered and then stabilized to a final hexagonal cylindrical structure upon increasing of curing temperature. Accordingly, a key aspect in the formation of these self-assembled structures, during the fabrication of ordered mesoporous phenolic resins, is the curing step (or cross-linking step). In other words, a mechanism involving reaction-induced microphase separation can be used to control the structure of the final product. In addition, in situ FTIR spectroscopy and DSC analyses of the cross-linked systems provided important evidence regarding the distribution of the cured phenolic resin in the whole mixed

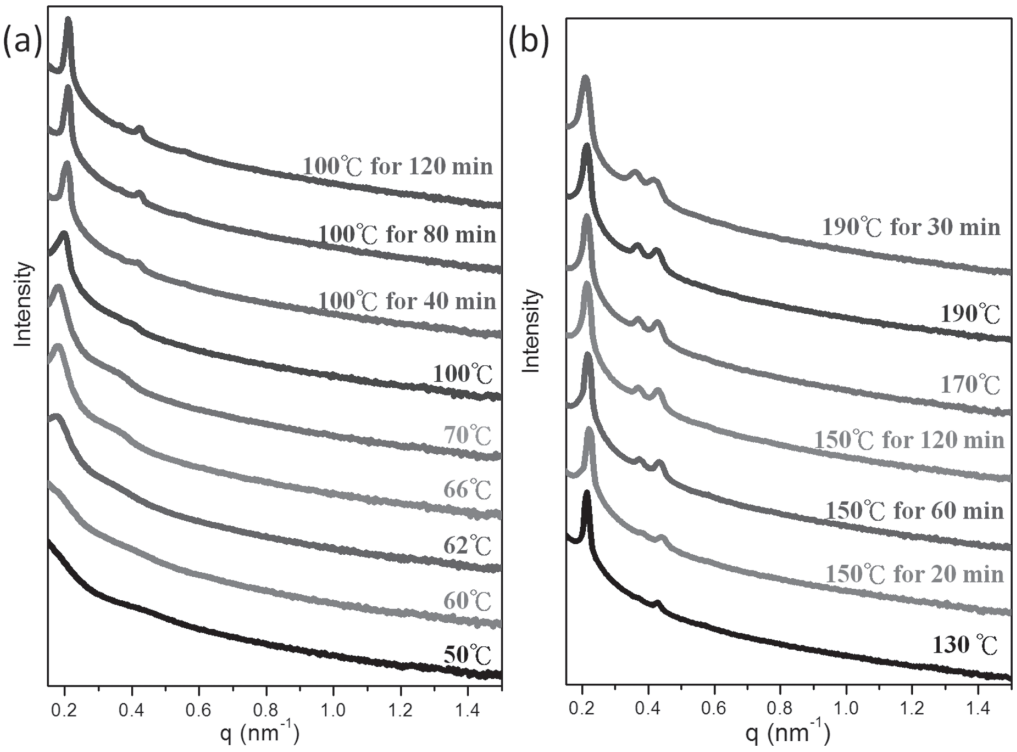

Figure 6. In situ SAXS patterns of the phenolic resin/PEO-*b*-PCL/PEO-POSS mixture during the curing reaction.

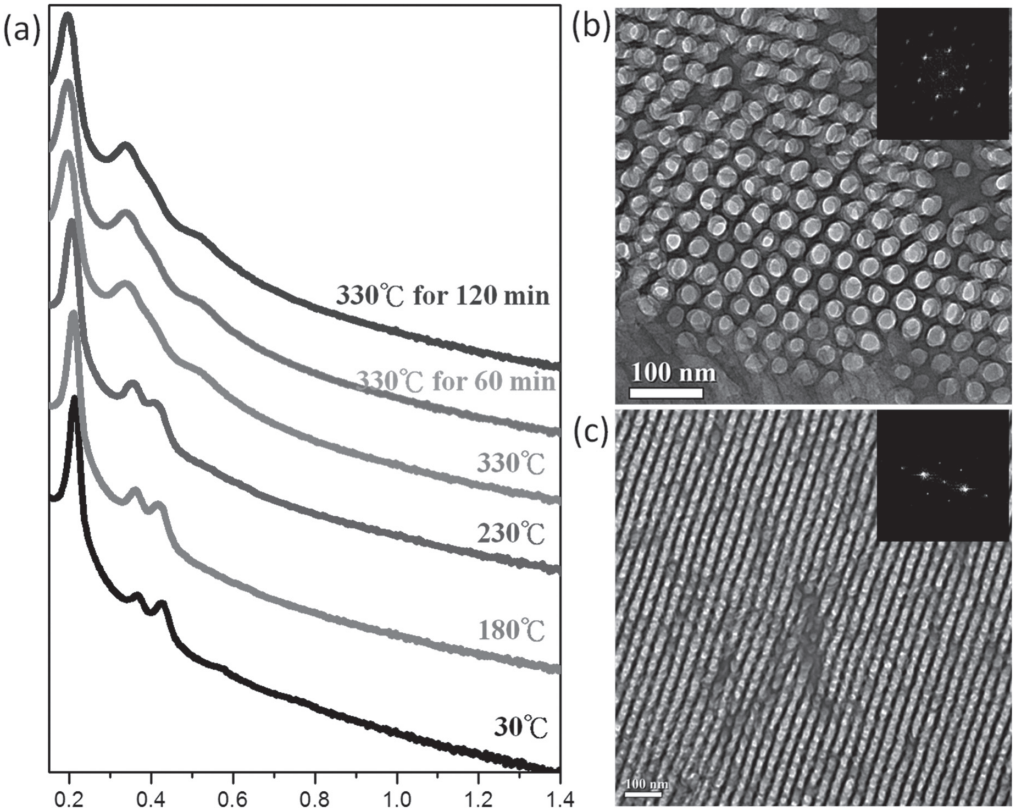

Figure 7. a) In situ SAXS patterns of the cured phenolic resin/PEO-*b*-PCL/PEO-POSS mixture during the calcination process. b,c) TEM images of the hexagonal cylindrical mesoporous phenolic resin viewed along the [001] and [10] planes, respectively.

system during the reaction-induced self-assembly process. Although we have described a fundamental study of the inner workings of only phenolic resin/PEO-*b*-PCL blends during their curing process, we believe that the concepts described herein could be applied to the preparation of mesoporous phenolic resins with different structures and, furthermore, to controlling the structures of mesoporous phenolic resins with focus on their ultimate applications.

Acknowledgements: This study was supported financially by the National Science Council, Taiwan, Republic of China, under contracts NSC 100–2221-E-110–029-MY3 and NSC 100–2628-E-110–001.

Received: May 1, 2013; Revised: June 3, 2013; Published online: July 24, 2013; DOI: 10.1002/macp.201300332

Keywords: block copolymers; microphase seperation; hydrogen bonding; in situ small-angle X-ray scattering (SAXS); mesoporous materials

[1] I. Muylaert, A. Verberckmoes, J. De Decker, P. Van der Voort, *Adv. Colloid Interface Sci.* **2012**, *175*, 39.
[2] Y. Wan, Y. F. Shi, D. Y. Zhao, *Chem. Mater.* **2008**, *20*, 932.
[3] J. G. Li, C. Y. Chung, S. W. Kuo, *J. Mater. Chem.* **2012**, *22*, 18583.
[4] J. G. Li, S. W. Kuo, *RSC Adv.* **2011**, *1*, 1822.
[5] J. G. Li, Y. D. Lin, S. W. Kuo, *Macromolecules* **2011**, *44*, 9295.
[6] F. Q. Zhang, Y. Meng, D. Gu, Y. Yan, C. Z. Yu, B. Tu, D. Y. Zhao, *J. Am. Chem. Soc.* **2005**, *127*, 13508.
[7] H. Kosonen, S. Valkama, A. Nykanen, M. Toivanen, G. ten Brinke, J. Ruokolainen, O. Ikkala, *Adv. Mater.* **2006**, *18*, 201.
[8] S. Valkama, A. Nykanen, H. Kosonen, R. Ramani, F. Tuomisto, P. Engelhardt, G. ten Brinke, O. Ikkala, J. Ruokolainen, *Adv. Funct. Mater.* **2007**, *17*, 183.
[9] Y. H. Deng, T. Yu, Y. Wan, Y. F. Shi, Y. Meng, D. Gu, L. J. Zhang, Y. Huang, C. Liu, X. J. Wu, D. Y. Zhao, *J. Am. Chem. Soc.* **2007**, *129*, 1690.
[10] Y. Fang, D. Gu, Y. Zou, Z. X. Wu, F. Y. Li, R. C. Che, Y. H. Deng, B. Tu, D. Y. Zhao, *Angew. Chem. Int. Ed.* **2010**, *49*, 7987.
[11] X. L. Ji, K. T. Lee, R. Holden, L. Zhang, J. J. Zhang, G. A. Botton, M. Couillard, L. F. Nazar,*Nat. Chem.* **2010**, *2*, 286.
[12] J. S. Lee, X. Q. Wang, H. M. Luo, G. A. Baker, S. Dai, *J. Am. Chem. Soc.* **2009**, *131*, 4596.
[13] X. Zhuang, Y. Wan, C. M. Feng, Y. Shen, D. Y. Zhao, *Chem. Mater.* **2009**, *21*, 706.
[14] M. Sevilla, A. B. Fuertes, *Carbon* **2006**, *44*, 468.
[15] L. Y. Song, D. Feng, N. J. Fredin, K. G. Yager, R. L. Jones, Q. Y. Wu, D. Y. Zhao, B. D. Vogt, *ACS Nano* **2010**, *4*, 189.
[16] J. G. Li, T. S. Lee, K. U. Jeong, C. H. Lin, S. W. Kuo, *RSC Adv.* **2012**, *2*, 11242.
[17] Y. Meng, D. Gu, F. Q. Zhang, Y. F. Shi, L. Cheng, D. Feng, Z. X. Wu, Z. X. Chen, Y. Wan, A. Stein, D. Y. Zhao, *Chem. Mater.* **2006**, *18*, 4447.
[18] N. P. Wickramaratne, M. Jaroniec, *Carbon* **2013**, *51*, 45.
[19] D. Hu, Z. G. Xu, K. Zeng, S. X. Zheng, *Macromolecules* **2010**, *43*, 2960.
[20] R. L. Liu, Y. F. Shi, Y. Wan, Y. Meng, F. Q. Zhang, D. Gu, Z. X. Chen, B. Tu, D. Y. Zhao, *J. Am. Chem. Soc.* **2006**, *128*, 11652.
[21] C. D. Liang, S. Dai, *J. Am. Chem. Soc.* **2006**, *128*, 5316.
[22] H. Y. Byun, M. H. Choi, I. J. Chung, *Chem. Mater.* **2001**, *13*, 4221.
[23] P. P. Chu, H. D. Wu, *Polymer* **2000**, *41*, 101.
[24] Y. Huang, J. P. Yang, H. Q. Cai, Y. P. Zhai, D. Feng, Y. H. Deng, B. Tu, D. Y. Zhao, *J. Mater. Chem.* **2009**, *19*, 6536.
[25] H. Kosonen, J. Ruokolainen, P. Nyholm, O. Ikkala, *Macromolecules* **2001**, *34*, 3046.
[26] G. Soler-Illia, E. L. Crepaldi, D. Grosso, C. Sanchez, *Curr. Opin. Colloid Interface Sci.* **2003**, *8*, 109.
[27] D. Grosso, F. Cagnol, G. Soler-Illia, E. L. Crepaldi, H. Amenitsch, A. Brunet-Bruneau, A. Bourgeois, C. Sanchez, *Adv. Funct. Mater.* **2004**, *14*, 309.
[28] Y. Wan, Y. F. Shi, D. Y. Zhao, *Chem. Commun.* **2007**, 897.
[29] W. C. Chu, J. G. Li, S. W. Kuo, *RSC Adv.* **2013**, *3*, 6485.
[30] S. W. Kuo, C. L. Lin, F. C. Chang, *Macromolecules* **2002**, *35*, 278.
[31] M. M. Coleman, P. C. Painter, *Miscible Polymer Blend-Background and Guide for Calculations and Design*, DEStech Publications, Inc., Lancaster, PA, USA, **2006**.
[32] H. L. Chen, J. C. Wu, T. L. Lin, J. S. Lin, *Macromolecules* **2001**, *34*, 6936.
[33] J. Y. Hsu, I. F. Hsieh, B. Nandan, F. C. Chiu, J. H. Chen, U. S. Jeng, H. L. Chen, *Macromolecules* **2007**, *40*, 5014.